

Experimental and numerical modelling of the flow field in a Cu_xSn_y direct chill caster

S. Eck^{*1}, C. Pfeiler¹, F. Mayer¹, A. Ludwig¹ and J. W. Evans²

To investigate the influence of the casting speed on the flow field and the shape of the solidification front in an industrial bronze caster, numerical calculations have been performed and experimental flow field measurements were used to validate the numerical model. Both numerical and experimental model represented 1:1 the real caster geometry of 820 × 250 × 800 mm³. A steady-state calculation, considering solidification and turbulent flow, was performed. Furthermore, a 1:1 water model of the industrial bronze caster has been built and combined with a Particle Image Velocity (PIV) setup to measure the apparent flow fields. Amongst other parameters, the numerical model provided information on the influence of the casting speed on the solidification front shape. The water model gave the experimentalist the facility to adjust the shape of the solidification front to the one predicted by the numerical model and compare the resulting flow field with the numerical prediction. This work presents a comparison of the results of both numerical and experimental models for different casting speeds with the same numerical parameters and boundary conditions.

Keywords: Copper, Bronze, Casting, Water model, Solidification, Experimental and numerical

Introduction

In the casting of real metals the opacity of the melt and the high temperatures involved make it difficult to measure, or even observe, the flow patterns resulting from different metal delivery devices. Consequently, mathematical and physical modelling have been extensively used to determine the flows in casters, particularly those of steel casters. While mathematical models have been widely accepted, their performance has frequently been judged by their ability to predict flows measured in physical (water) models.^{1–3} In the case of steel casting, physical modelling of the flow fields in the liquid melt is often performed by using water models and Particle Image Velocimetry (PIV) or similar flow field measurement techniques. The most interesting region for this type of investigation is the region near the nozzle and industrial research groups test new nozzle designs with PIV measurements near the submerged entry nozzle. The physical models referred to generally either ignore the formation of the solidification front or just take it into account by changing from a purely cylindrical geometry to a conical geometry. For steel casting this is a good approximation because the final solidification point, i.e. the point where the casting product is fully solidified is several meters away from the submerged entry nozzle.^{2,3} There are, however, other metals and alloys where the solidification front is much

closer to the entry nozzle and this has therefore to be taken into account in both numerical and experimental modelling of the casting process. Xu *et al.*⁴ have shown that in the case of Al direct chill casting the distance between entry of the liquid metal and the solidification front is in the order of 0.4 m. Recent calculations and cooperation with industrial partners revealed that in the case of Cu based alloys this distance is of the same order of magnitude.^{5–7} Therefore, if a physical model of the flow fields appearing in these casting processes is to be realistic, it has to include the distance and shape of the solidification front. In real casting the shape of the solidification front depends on the casting material constants like heat transfer coefficient, viscosity, and density and on the casting parameters such as casting speed, cooling geometry and cooling efficiency. In a previous publication the authors showed how the flow in a real industrial bronze caster was modelled by a water model.⁸ In this case an experimentally determined solidification front shape for a given casting velocity had been modelled by a flexible ‘solidification front module’ in the water model. The aims of the present investigations were to use numerical simulations of the same caster to show the influence of the casting speed on the shape of the solidification front, to adapt the solidification front module of the water model according to the predicted shapes and to compare the resulting flow fields of the water model with the numerical predictions for bronze.

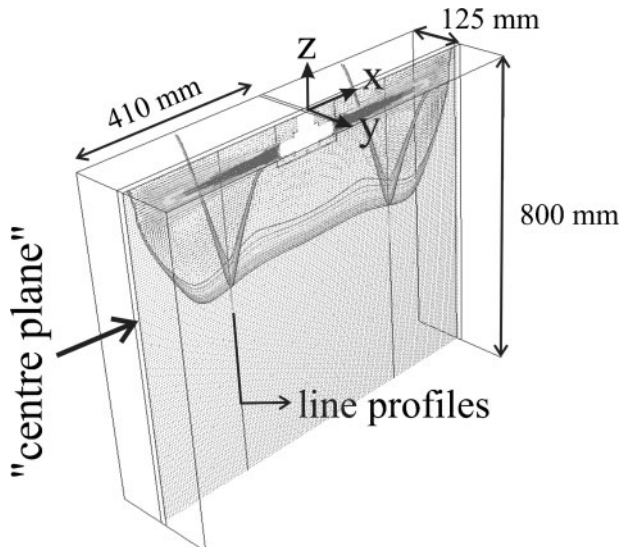
Numerical model: geometry, grid and boundary conditions

For the numerical simulation the industrial caster dimensions of 820 × 250 × 800 mm were simplified by

¹Chair for Simulation and Modelling of Metallurgical Processes (SMMP), Dept. Metallurgy, University of Leoben, A-8700 Leoben, Austria

²Chair for Mineral Engineering, Mat. Sci. & Eng. Dept. University of California, Berkeley, CA-94720, USA

*Corresponding author, emails sven.eck@mu-leoben.at



1 Illustration of the calculated domain modelling the industrial bronze caster with 2 symmetry planes x-z and y-z. The wide symmetry plane was referred to as the 'centre plane'

assuming two vertical symmetry planes, thus one quarter of the real geometry was calculated. Fig. 1 illustrates the 3D domain, its dimensions and the position of the centre plane that will be referred to in the following sections. As reported elsewhere,⁸ the inlet geometry was that of an inverted T with a 130 mm long horizontal cylindrical inlet of 26 mm diameter that was submerged by 50 mm below the top of the liquid pool. To model the cylindrical inlet, a fine polyhedral mesh around the inlet region was combined with a coarser hexagonal mesh for the remaining geometry. The resulting 3D mesh for the 410 × 125 × 800 mm³ domain consisted of 280 000 cells. To calculate the flow fields and the shape of the solidification front, the commercial CFD package FLUENT⁹ was used. To model the turbulent flow field, the realizable $k-\epsilon$ model⁹ has been applied, to calculate the solidification front shape, FLUENT's integrated solidification module has been applied. The following boundary conditions have been set: 'Free slip' and no heat transfer at the top, 'moving wall' with no slip and a heat transfer coefficient of 3000 W/m²K at the vertical walls, pressure inlet at the nozzle and a velocity outlet corresponding to the casting speed at the bottom. The temperature of the incoming melt was set to 1390 K, i.e. 100 K above the liquidus temperature assumed for an industrial bronze alloy; other relevant material properties were taken from a freely available on-line source.¹⁰

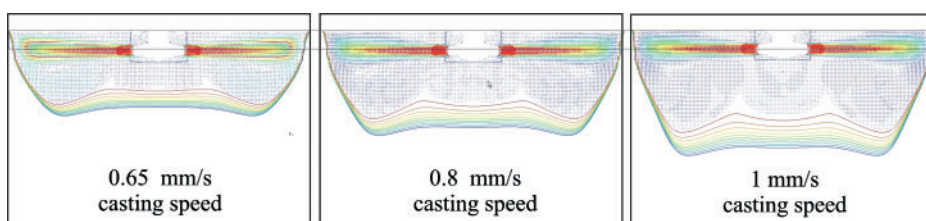
Calculated solidification front shapes for different casting speeds

To estimate the influence of the casting speed on the flow and the solidification front shape, the 3 different casting speeds 0.65 mm/s, 0.8 mm/s and 1 mm/s have been calculated. The results of these calculations have been plotted in the centre plane as velocity vectors combined with lines representing liquid fractions f_l ranging from 0.9 to 1. The results are presented in Fig. 2 and showed how the sump depth increased with increasing casting velocity. Two vortices of the melt flow developed that were driven by the downwards flow where the incoming jet hits the wall and the resulting upwards flow in the centre. As the incoming melt was hotter than the liquid pool, the vortices generated a W-shape of the solidification that became more pronounced with increasing casting speed, i.e. increasing jet velocity.

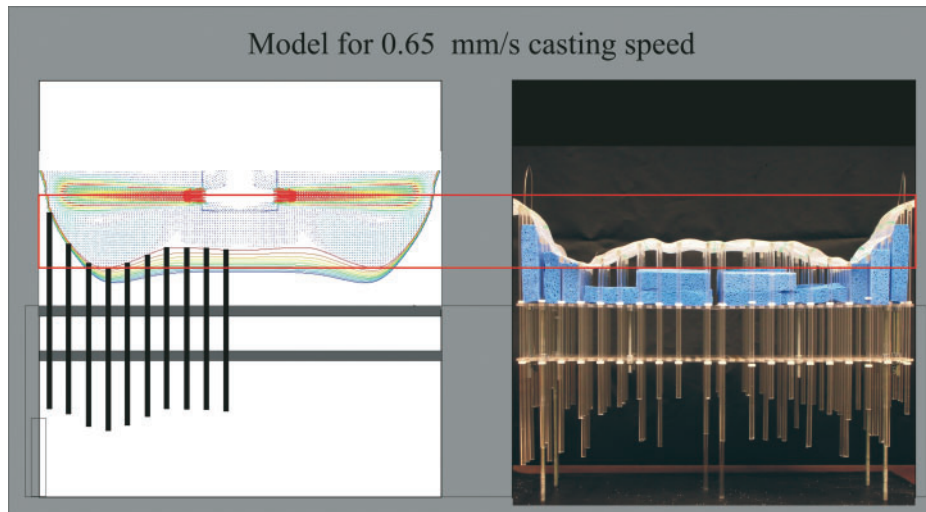
Experimental model and results

When comparing the flow in liquid metal and in water and based on the simplifications of isothermal flow, the Reynolds number $Re=V L/v$ has to be constant, where V is the mean fluid velocity, L is the characteristic length and v is the kinematic fluid viscosity. For the modeled casting process, the casting speed determined the flow rate Q , e.g. for 1 mm/s casting speed the flow rate was $Q=0.82 \text{ m} \times 0.25 \text{ m} \times 0.001 \text{ m s}^{-1}=2.05 \times 10^{-4} \text{ m}^3 \text{ s}^{-1}$. The velocity at the inlet of the water model is then linked to the flow rate by the area of the inlet. For the 1:1 model, the characteristic lengths were constant, thus the water velocity (and the flow rate) only had to be scaled by the ratio of the kinematic viscosities of liquid bronze and water to keep the Reynolds numbers constant.

The basic setup of the experimental water model and the PIV measurement has been described in a previous publication.⁸ There, a comparison of the results of both numerical and experimental models for the water flow without the solidification front module showed a good agreement both in the qualitative velocity fields and in the quantitative comparison of the velocity profiles along vertical lines. It has been shown that PIV vector maps that had been time averaged over more than 5 sec showed a stable flow field that could be compared with steady state CFD calculations.⁸ First experimental results of the flow field obtained with a solidification front and inlet conditions as provided by the Cu alloy manufacturing company showed that the solidification front module itself had to be improved in order to better reflect the resistance of the mushy zone and the solid to the flow. Consequently, a new solidification front module has been designed that allowed a quicker and more accurate adjustability of the solidification front



2 Velocity vectors and liquid fraction lines f_l (0.9 to 1) in the centre plane calculated for 3 different casting speeds



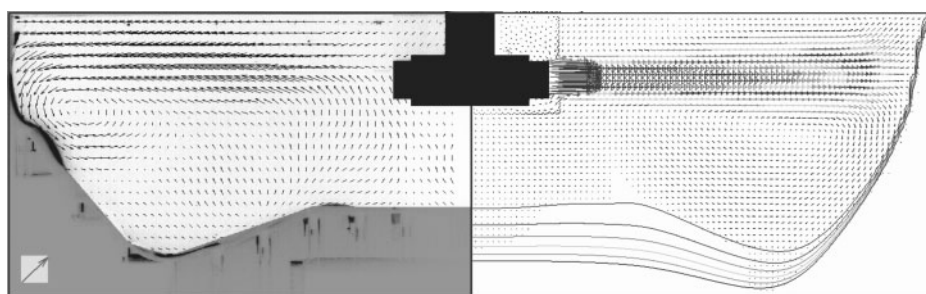
3 The solidification front module for 0.65 mm/s casting speed (right side) based on the numerical calculation (left side), superimposed with the design sketch for the vertical rods that hold the solidification front mesh

shape. Figure 3 shows how the calculated solidification front has been taken to adjust the new solidification front module, in this case for 0.65 mm/s casting speed. In the previous investigations⁸ it had been observed that in the region where the inlet jet hit the wall the velocities pointed downwards into the mesh rather than being parallel to it. This indicated that in this region of the solidification front module the mesh was not sufficient to model the higher resistance to the flow due to the higher solid fraction of the real mushy zone in that region. To improve the model also in that respect, sponges have been added below the mesh near the wall to block the downward flow in that region. Further sponges have been added in the centre region but showed only minor effects on the flow as the flow velocities were much lower in that region and almost parallel to the mesh.

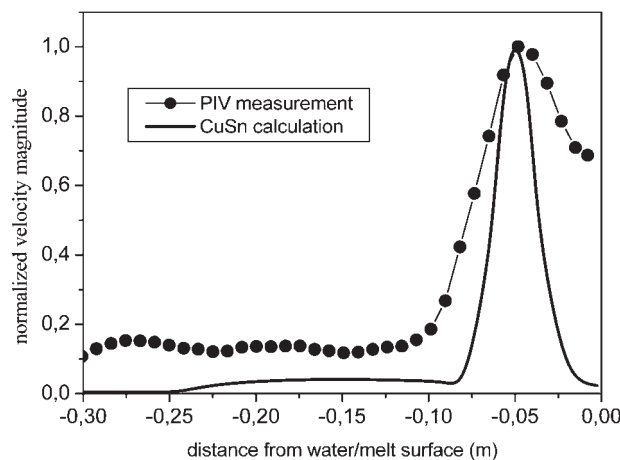
Comparison of the flow fields

In Fig. 4 we present a direct comparison of the measured (left) and the calculated flow fields for 0.65 mm/s casting speed. Note that the numerical and the experimental evaluation inherently showed different numbers of velocity vectors. Furthermore, an auto scaling of the length of the velocity vectors was used on both sides for a better comparison of the different flow fields measured for water and computed for bronze. The same type of comparison has been elaborated for 0.8 and 1 mm/s

(results not shown). Both numerical and experimental velocity fields show an inlet jet that was slightly tilted upwards and a strong vortex below the region where the jets hit the wall. Regions of very low velocities were measured and calculated right below and above the inverted T shape nozzle. The experimental results showed lower velocities near the inlet than in the region at about half the distance to the wall. These low velocities are attributed to a PIV measurement error: the low seeding of the incoming water in that region led to fewer measured velocities that in combination with the applied statistics over 10 s (500 PIV maps) generated lower velocities. Apart from these discrepancies the experimental and numerical results showed a good qualitative agreement for all three casting velocities, i.e. in the direction of the velocity vectors and the appearance of vortices. For a quantitative comparison of the results vertical line profiles (velocity magnitude versus z-position) have been exported at 205 mm distance from the left wall ($x=205$, $y=0$). The position of this line in the experimental setup is indicated in Fig. 1. For a direct comparison the resulting velocity line profiles had to be normalized for two reasons: First, the water flow velocity had been scaled by the ratio of the kinematic viscosities of liquid bronze and water to keep the Reynolds numbers constant, thus the velocities in the water model were by a factor of 2.2 higher than the calculated bronze velocities. Second, the PIV results represent the velocities in the illumination plane, in this setup an approx. 10 mm wide plane, whereas the



4 Qualitative comparison of measured and calculated flow fields for 0.65 mm/s bronze casting velocity; left: 10 s time-averaged PIV measurement for a water model with adjusted flow rate and solidification front; right: CFD steady state calculation for bronze. Note that the numerical and the experimental evaluation programs inherently showed different numbers of velocity vectors and an auto scaling of the length of the velocity vectors was used on both sides



5 Normalized velocity line profiles along the vertical line shown in Fig. 1, dots: PIV measurement in the water model; line: CFD calculation for bronze

FLUENT results had been extracted from a numerical ideal thin plane. As the latter influence could not be described by a simple multiplication factor, the maximum jet velocity was taken for the normalization, i.e. it was normalized to 1 for both the experimental and the numerical line profile. The direct comparison of the velocity line profiles as shown in Fig. 5 revealed that the computed bronze jet was narrower than the measured water jet and that the velocities in the region below the jet were measured at higher values than predicted by the numerical model. Both facts can be interpreted as the kinetic energy of the jet in the water model dissipating more slowly than predicted. The realizable k - ε turbulence model had been applied because in comparison to the standard k - ε turbulence model it predicts the spreading rate of round jets more accurately.⁹ The discrepancies in the line profiles indicate that the values for the turbulence kinetic energy k and its dissipation rate ε at the inlet have to be adjusted to improve the predictions of the liquid bronze flow during the casting process.

Summary

To investigate the influence of the casting speed on the flow field and the shape of the solidification front in an industrial bronze caster, numerical calculations have

been performed and experimental flow field measurements in a 1:1 water model with an adjustable solidification front module were used to validate the numerical model. A comparison of the results of both numerical and experimental models for the flow during the casting process showed a good agreement in the qualitative velocity fields; i.e. both models showed the same flow directions and the same development and position of vortices in the flow field. The observed discrepancies in the quantitative comparison of the velocity profiles along vertical lines will be taken as source and guidance for the optimization of the numerical model.

Acknowledgements

This work was mutually funded by the Austrian Science funds (FWF) through means of the Erwin Schrödinger fellowship J2602 ‘Physical Modelling of Cu-Sn Casting’, the University of Leoben, Austria and the P. Malozemoff Chair in Mineral Engineering at the Department of Materials Science and Engineering of the University of California Berkeley, CA.

References

1. J.W. Evans: ‘Computational fluid dynamics in Mineral & Metals Processing and Power Generation’, CSIRO, Clayton, Victoria, Australia, 1997, 7–20.
2. H. Bai and B.G. Thomas: *Metall. Mater. Trans. B*, 2001, **32B** (2), 253–267.
3. Brian G. Thomas, Quan Yuan, S. Sivaramakrishnan, and S. P. Vanka: *JOM-e*, 2001, **54**, (1).
4. D. Xu, W. Kinzy Jones, J. W. Evans: *Metall. Mater. Trans. B*, 1998, **29B**, 1281.
5. Wieland-Werke AG, Graf Arco-Str. 36, 89079 Ulm, Germany, communications.
6. A. Ludwig, M. Gruber-Pretzler, F. Mayer, A. Ishmurzin, M. Wu: *Mat. Sci. Eng. A*, 2005, **413-414**, 485–489.
7. M. Gruber-Pretzler, F. Mayer, M. Wu: A. Ludwig, ‘Continuous Casting’, 2006; Ed. H. R. Müller, Germany, Wiley-VCH, ISBN-13: 987-52731341-9, 219–225.
8. S. Eck, A. Ludwig, D. Mazumdar and J.W. Evans: Proceedings of the 5th Decennial Conference on Solidification Processing, Sheffield, July 2007, University of Sheffield, 487.
9. FLUENT 6.0 user’s guide, FLUENT Inc., Lebanon, NH, USA.
10. MatWeb on-line. Material property database, <http://www.matweb.com>